

Unveiling the origin of oxygen atomic impurities in Au nanowires

A. P. F. Nascimento,¹ Miguel A. San-Miguel,² and E. Z. da Silva¹

¹*Institute of Physics “Gleb Wataghin,” University of Campinas–Unicamp, 13083-970 Campinas, SP, Brazil*

²*Department Physical Chemistry, University of Seville, 41012 Seville, Spain*

(Received 23 July 2013; revised manuscript received 23 January 2014; published 20 February 2014)

The appearance of unusually large Au-Au bond distances in linear atomic chains (LACs) of Au nanowires is commonly attributed to the presence of atomic impurities. However, the origin of those contaminants is unknown. We present a study based on density functional theory calculations using quasistatic ($T = 0$) and finite-temperature *ab initio* molecular-dynamics simulations of a possible route for the formation of atomic impurities in Au nanowires. This process starts with the adsorption of an O₂ molecule followed by a CO molecule on Au LACs, leading to the formation of an intermediate O₂CO complex. Upon thermal activation at finite temperatures, the complex is able to proceed to oxidation forming a CO₂ molecule and leaving an atomic O impurity in the Au LAC.

DOI: [10.1103/PhysRevB.89.085417](https://doi.org/10.1103/PhysRevB.89.085417)

PACS number(s): 31.15.A–, 62.23.Hj, 82.30.–b, 87.15.hp

I. INTRODUCTION

One of the very exciting achievements of nanoscience, at the turn of the 20th century, was the fabrication of very thin suspended gold nanowires with interesting properties [1]. Experiments in the subsequent years showed the production of thin nanowires (NWs) as thin as a linear atomic chain (LAC) with 4–10 atoms [2–4]. Theory and simulations also produced the evolution of thin NWs showing the formation of LACs [5–8]. These nanostructures present avenues of research with interesting possibilities as nanocircuits, filters, and catalysts.

The observation of large bond distances in LAC NWs, around 3.6 Å, intrigued researchers [1,2,4]. Several computational studies on Au NWs failed to find such long bond lengths in pure Au NWs [5,6,8]. Experimentalists and theoreticians started to look for foreign agents to explain such large bond lengths, and light atomic impurities were considered to be the reason for the large distances. Electron microscopy, used to image Au NWs, was unable to “see” these small atoms due experimental difficulties of contrast. In the other front, theoreticians were able to ask and answer these questions with the study of the effect of impurities in the LAC of these NWs [9–12]. This line of research has contributed interesting effects, such as the case of oxygen (O) atomic impurities, proposed as clamps that aid the production of longer LACs in Au NWs [13]. Theoretical predictions [13] were experimentally verified [3,4]. The reason for the consideration of impurities comes from the fact that even in ultrahigh vacuum used in the experiments, the chamber always contains molecules such as O₂, CO, CO₂, and H₂O, among others [4]. It might be possible that these molecules would contribute somehow to the formation of the single atom impurities. One question remains a mystery: what is the origin of these atomic impurities, and how do they end up in the LAC? The present article gives a possible answer to this experimental question of the formation of single impurities, and for this reason we investigate Au NWs with LACs of three and four atoms and the routes for the formation of these atomic impurities.

Gold is well known for its nonreactivity, being one of the noblest metals, when in bulk form. As sizes decrease and Au nanostructures are considered, it can become a good catalyst. Since the work of Haruta [14] that showed CO

oxidation catalyzed by supported gold nanoclusters, intense research considered Au nanoclusters as important catalysts [15]. According to Huchings and Haruta [16], the importance of gold as a good catalyst is due to the discovery showing that supported Au nanoparticles are very active for low-temperature CO oxidation [14]. In the search for hydrogen oxidation, they found that composite oxides of gold with some transition metals of group VIII (Fe, Co, and Ni) were much more active for CO oxidation than for H oxidation. Later it was found that these gold composites were gold nanoparticles on oxide supports such as Fe₂O₃, Co₃O₄, or NiO. Further studies concluded that the nanoparticle size is crucial to the catalytic activity [17]. Another influence on the oxidation is the type of support of the gold nanoclusters, e.g., TiO₂, Co₃O₄, and Fe₂O₃ [18]. Also, the preparation conditions are very important because they can affect the final shape of the nanoclusters [19]. Theoretical attempts to understand the CO oxidation mechanisms were undertaken [20–24]. These works tried to find the best scenarios for the reactions to take place. More recently, new and interesting results were published in the case of adsorption of O₂ in Au clusters supported in MgO film. This work showed the formation of one-dimensional gold oxide at the perimeter of the Au nanocluster, with new O states favoring CO oxidation [25]. Thus, nanoclusters supported on surfaces have long been targeted from experimental and computational techniques since they expose metal atoms in a wide range of geometrical configurations and low coordination numbers. At times the catalytic role played in different processes has been elucidated, but there are still open questions in this area of research.

Small molecules that exist in the atmosphere, such as H₂, O₂, CO, CO₂, and H₂O, do not react with Au. Au nanostructures, on the other hand, exhibit reactivity, and Au nanoclusters have been extensively studied in the role of catalysts. Many experiments on Au NWs, such as high-resolution transmission electron microscopy (HRTEM) experiments, work in ultrahigh vacuum, but even in these clean environments, the chamber always contains some of these small molecules [4]. This fact, along with the reactivity of Au nanostructures other than nanowires, was the reason for the study of the effect of O₂ and CO molecules in the gas phase approaching the Au LAC. The present systems, namely Au NWs, offer opportunities

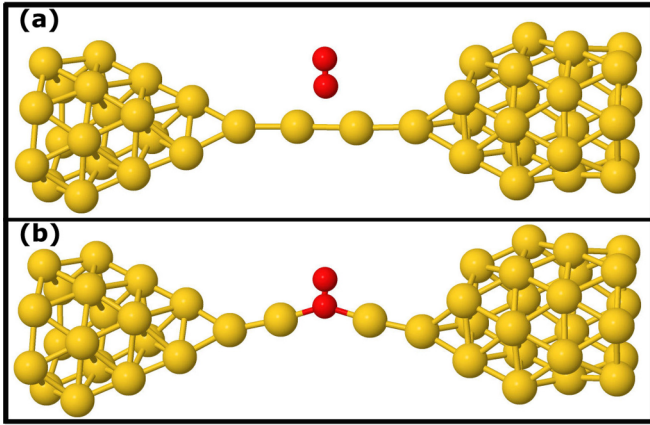


FIG. 1. (Color online) Formation of the Au-O₂ complex. (a) Pure nanowire with a four-atom linear chain and an O₂ molecule in the gas phase nearby. (b) The final stable nanowire with the Au-O₂-Au complex.

in this regard, since the reactions studied occur at the linear atomic chain of the NW (see Fig. 1), where LAC atoms are very low coordinated (two Au neighbors) and it is possible to control their bond lengths in experiments such as mechanically controllable breaking junctions (MCBJ) [26]. This control is in fact an important factor for the O₂ reaction that in the present case can be driven by mechanical or thermal effects, as will be explained later. Although this work is not aimed at developing a new catalytic process, it presents a pathway involving the CO oxidation promoted by Au LACs, causing the insertion of single impurities in these LACs and therefore explaining the origin of the unusual large distances.

This paper presents a possible route to the formation of a single atomic impurity in Au NWs. To address this problem, NWs with LACs of four atoms are used. The reason is that they correspond to the initial situation encountered in the experiments [4], where it appears that pure Au NWs with chains of around four atoms may adsorb impurities such as O, which was shown to help the formation of longer LACs [13].

Section II discusses the methodology employed to perform the present study. Then, Sec. III uses the methodology to discuss a chemical route that leads to the formation of an atomic impurity in the Au LAC. This is the case for the formation of an O impurity, which is of particular interest since O was previously singled out as an agent that helps the formation of longer Au LACs [3,4,13]. This article details this process and lifts the mystery of the origin of the O atomic impurity in Au-LAC NWs, providing an oxidation route facilitated by the catalytic contribution of the Au-LAC. Finally, Sec. IV presents the conclusions of this work, along with some possible applications of this process.

II. METHODS

Our results are based on DFT calculations [27,28]. All calculations used the generalized gradient approximation (GGA) functional under the Perdew-Burke-Ernzerhof (PBE) implementation [29] and norm-conserving pseudopotentials [30]. The pseudopotentials included the 2*s* and 2*p* orbitals for O and C and 5*d* and 6*s* for Au [31,32], using the SIESTA code.

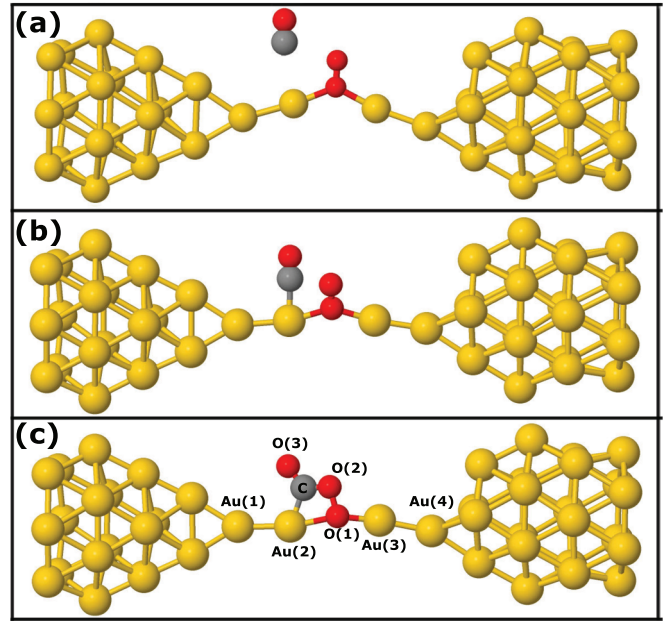


FIG. 2. (Color online) Formation of the Au-O₂CO complex. (a) The O₂ molecule with one O atom attached to two Au LAC atoms and also a CO molecule nearby. (b) The CO molecule adsorbing to one Au atom [Au(2)] that has one Au-O bond. (c) The final stable Au-O₂CO complex.

The calculations used numerical orbitals as basis sets [33]; all atoms were described by a split valence double-zeta basis with polarization function (DZP). A supercell was defined with periodic boundary conditions to define a chain geometry, including a vacuum space of 30 × 30 Å in the perpendicular directions to the chain to avoid interaction between the NW and its images. The Brillouin zone sampling used the Monkhorst and Pack *k*-points (eight points along the NW direction) [34]. The *T* = 0 electronic structure calculations were performed using the conjugate gradient (CG) method, in which all force components were smaller than 0.007 eV/Å.

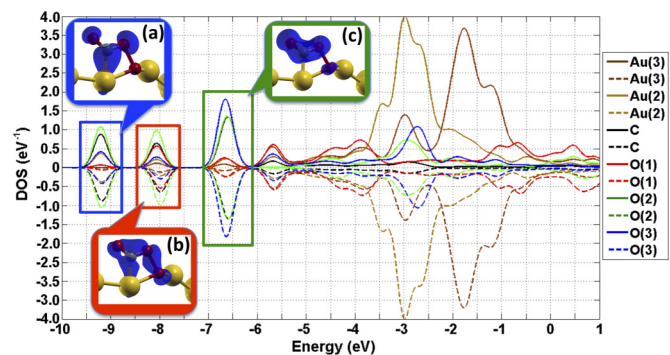


FIG. 3. (Color online) Density of states (DOS) of the O₂CO complex. Insets are representative total electron density for the O₂CO complex at specific DOS intervals corresponding to (a) σ donation from the C to the metal, (b) π backdonation from Au *d* orbitals to the empty C *p* orbitals, and (c) σ bonds between C and O atoms. Isosurfaces are of 0.01 electrons/(Bohr)³. Continuum lines denote spin α and dashed lines denote spin β .

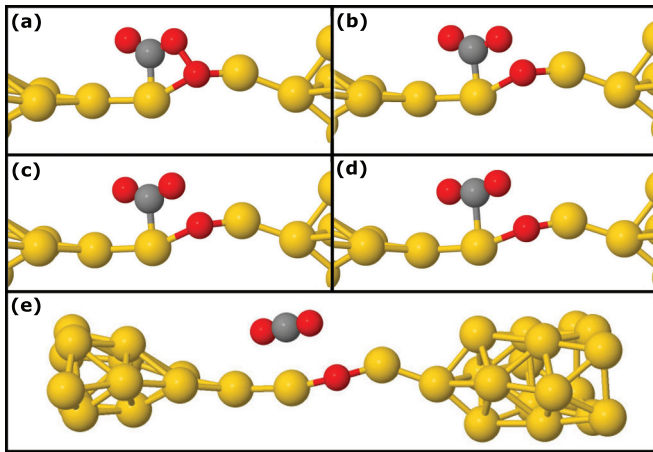


FIG. 4. (Color online) Formation of a CO_2 molecule that goes into the gas phase, leaving an atomic O in the Au NW. (a) The stable complex at an intermediate stage. (b) Breaking of the O_2 bond, the starting of the formation of the CO_2 molecule. (c) The Au-C distance increases and the CO_2 opens its angle. (d) Breaking of the Au-C bond with the formation of a gas phase CO_2 . (e) Au NW with O atomic impurity and CO_2 in gas phase.

The confining energy shift was 0.07 eV. The cutoff for the grid integration was 300 Ry for the CG calculations and 250 Ry for the molecular-dynamics simulations. *Ab initio* molecular dynamics (AIMD) as implemented in SIESTA was used with a procedure similar to previous works [35,36]. The AIMD simulations were performed in the microcanonical ensemble with rescaling of temperature for a target temperature of 500 K [36]. The equations of motion were integrated by the velocity Verlet algorithm with a time step of 1 fs. The system was thermalized at 300 MD steps (not shown in the figures). The Au NWs with LACs of four atoms had 44 atoms for the CG calculations. The AIMD calculations of the evolution of the Au- O_2CO complex were done using a system containing 32 Au atoms. The two most external Au rings were removed to allow less time-demanding simulations as previously reported [36]. Tests showed that the behaviors of both systems are very similar. These structures came from previous works [5,6,13]. All snapshots presented in Figs. 1, 2, and 4 were produced using the open-source code JMOL [37].

III. RESULTS

The interaction of O_2 molecules with Au structures, namely Au nanoclusters, free or supported on surfaces, has been studied extensively but is not fully understood yet. In this work, we aim to gain insight into a different system. We focus on the O_2 interaction with thin Au NWs as a precursor for the formation of atomic O impurities that have been reported previously and theoretically studied. To find these sites, O_2 molecules were left at the vicinity of the Au NW. To achieve this goal, we considered Au NWs with linear atomic chains (LACs) of three and four atoms, and O_2 molecules at different positions close to the NW, both the tips and the atomic chain. In this work, only NWs with four atoms in the LAC are discussed. Figure 1(a) shows one of these NWs in which the bond length of the Au LAC atoms is on average 2.9 Å. Many studies of the

approach of an O_2 molecule were attempted, using both CG and AIMD. While O_2 attached to Au atoms at the tips, in the chain the stable position was between two Au atoms, bridging the bond and forming Au-O-Au (with the second O sticking out of the structure) or Au-O-O-Au structures. To find these sites, O_2 molecules were left at the vicinity of the Au NW. In the CG process, initially, O_2 molecules were placed 2.0 Å above the middle point of an Au-Au bond or above one Au atom and then the structure was allowed to relax. The most interesting cases were the O_2 adsorptions at the central point of the four atom LAC. Figure 1 shows the NW and the O_2 in the gas phase (frame 1) and the O_2 inserted in the central Au-Au LAC bond (frame 2). The NW was considered with different degrees of stress, which resulted in different Au-Au bond distances for the LAC atoms. As a result, many outcomes occurred. We found that NWs with little tension (Au-Au average distances of around 2.6 Å) do not adsorb O_2 molecules, presumably due to a lack of space in the Au-Au bonds. If the LAC is too stressed (Au-Au average distances longer than 2.9 Å), the O_2 molecule is inserted with both atoms, forming a peroxy structure Au-O-O-Au. The most interesting case is when the stress is moderate and Au-Au average distances are in the range of 2.7–2.9 Å. In those cases, the O_2 molecule is adsorbed into the LAC but only one O atom bonds to the Au-Au chain forming Au-O-Au bonds [Fig. 1(b) and also Fig. 2(a)]. This result was found using both CG calculations and AIMD simulations at $T = 300$ K. Figure 2(a) shows the final stage of the AIMD evolution of the O_2 molecule. A film (VIDEO-1 provided in the supplemental material [38]) illustrates the O_2 molecule approaching from the gas phase and the adsorption process to the Au LAC leading to the formation of a stable structure, which is the precursor of the next stage.

The initial process considered was the adsorption of an O_2 molecule on the LAC (Fig. 1), which turned out to be favorable (−0.89 eV). Further adsorption of a CO molecule is also favored (−1.92 eV), and it led to the formation of an O_2CO complex that upon activation proceeds to the oxidation and release of a CO_2 molecule.

The O_2 adsorption energy varies quite significantly with stress, which changes the average Au-Au LAC bond length. For average Au-Au distances of 2.7 Å, it is −0.41 eV (which is comparable with values reported by Yoon *et al.* [39]), while for Au-Au distances of 2.9 Å, it is −0.89 eV. This fact illustrates significant differences from nanowires with respect to surfaces and clusters in which the atom-atom distances are more restricted because of the three-dimensional arrangement. Thus, in nanowires those distances can be controlled by stress, opening new adsorption scenarios. In fact, CMBJ experiments can control the stress on the NW. Our simulations mimic this feature available in thin metal NWs.

A CO molecule can also be adsorbed on the LAC next to the O_2 -LAC forming a stable O_2CO complex. Upon activation mediated by mechanical deformations or thermal fluctuations, this complex follows an oxidation pathway forming a CO_2 molecule and leaving a single O atom inserted in the LAC. It is well known that the oxidation of CO is a process hindered by a high-energy barrier, and only catalytic activity allows that process to take place [40]. Most of the pathways proposed involve the presence of O adatoms which interact with the adsorbed CO forming the CO_2 [21]. It has also been

suggested that this oxidation reaction occurs in Au steps and Au clusters supported on MgO, through the formation of a metastable intermediate O₂CO complex [21,23] similar to the ones observed in our studies.

The stable structure depicted in Fig. 2(c) has some interesting features worth mentioning. It forms an α angle of 106° [see also the inset in Fig. 5(a)]. CG calculations with the complex rotated to an angle of 100.8°, which increased the O(1)-O(2) bond, made the complex unstable and led to the formation of a CO₂ molecule, leaving an O atomic impurity adsorbed in the LAC. If the energy barrier for this process is modest, it could occur due to thermal fluctuations. To verify this possibility, we performed AIMD simulations at 500 K. Therefore, the stable O₂CO complex obtained from CG calculations [Fig. 2(c)] was taken as input to AIMD simulations. After thermalization, the evolution of the structure as observed was indeed a concerted process that occurred in many different simulations. We shall describe in detail one of these processes at temperature 500 K.

The formation of the complex assisted by the NW occurs with no energy barrier when a CO molecule approaches the O₂-LAC [Figs. 1(b) and 1(c)]. The adsorption energy for this process is -1.92 eV. A typical density of states (DOS) of the complex showing the contribution of the most important atoms in the complex formation is depicted in Fig. 3. Details of bond formation are given in the insets (a), (b), and (c), where isosurfaces of the most important contribution to the bonding are presented.

The CO fragment in the O₂CO complex [see Fig. 2(c)] interacts with Au(2) involving σ donation from the C atom to the metal [Fig. 3, inset (a)] and simultaneously a π backdonation from Au *d* orbitals to the empty C *p* orbitals [inset (b) in Fig. 3]. In the complex, this Au(2)-C bond is weakened due to the formation of a new bond between the C atom and the O(2) in a characteristic *sp*² hybridization scheme. This weakens the Au(2)-O(1) bond and enlarges the O-O distance by around 0.2 Å of the peroxy bond. Inset (c) in Fig. 3 shows σ C-O bonds that will evolve to form the CO₂ molecule. The electron density contributions to these bonds in the O₂CO complex can be visualized from representative regions (depicted in colored boxes associated with the insets) in the DOS plot of Fig. 3. The DOS corresponds to the complex structure depicted in Figs. 2(c) and 4(a).

In the AIMD simulation, the O₂CO complex depicted in Fig. 4(a) stays stable for a period of time. When the O(1)-O(2) bond increases, a concerted process starts and the formation of CO₂ occurs rapidly. To verify this result, we also performed the AIMD simulation using a Nose-Hoover thermostat (as implemented in the SIESTA code) at the same temperature, and the reaction occurred similarly. In the supplemental material, videos (VIDEO-2, VIDEO-3, VIDEO-4) illustrate the reaction using both AIMD procedures.

Figure 4(b) shows a moment just after the breaking of the O(1)-O(2) bond. At this stage, similar to the effect observed in CG, the α -angle reached smaller values. The structure started to become unstable, the O(1)-O(2) and the Au(2)-C distances increased, and the Au(2)-O(1) bond was reestablished [Fig. 4(c)]. Next, the Au(2)-C bond increases further [Fig. 4(d)], and then the *sp*² bonds that hold the two O atoms to the C atom transform into *sp* bonds as the Au(2)-C

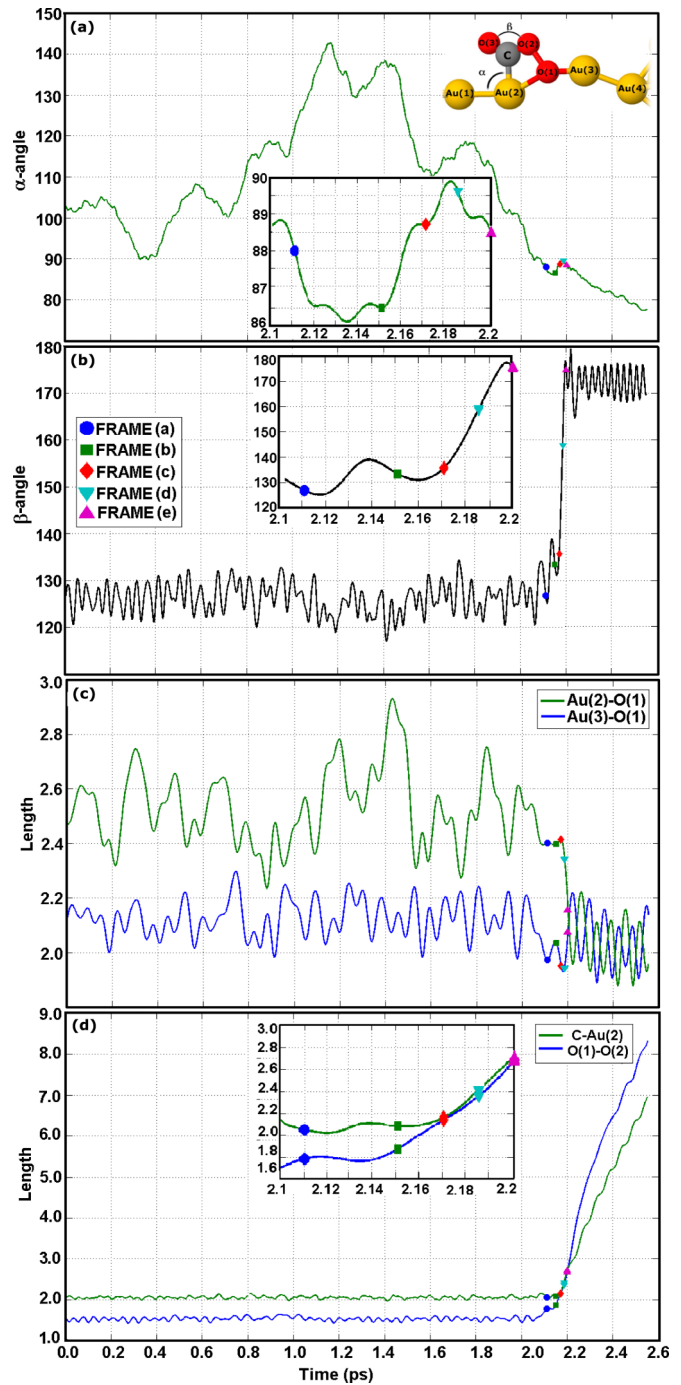


FIG. 5. (Color online) The MD simulation showing the time dependence of some particular bonds and angles. Five special points in colored symbols depict the selected five snapshots of Fig. 2 [named FRAME (a)–(f)]. They are highlighted in the insets. (a) The evolution of the α angle (inset of the NW structure, refers to angles and bonds depicted in the plots). (b) The evolution of the β angle. (c) The evolution of the Au(2)-O(1) and the Au(3)-O(1) bonds. (d) The evolution of the C-Au(2) and the O(1)-O(2) bonds.

bond breaks and the O-C-O structure transforms into a CO₂ molecule, which goes into the gas phase as seen in Fig. 4(e).

To prove the above statements, Fig. 5 shows the evolution of some important distances and angles along the AIMD

simulation. Graph (a) shows the evolution of the α -angle. It can be seen that under the fluctuations, this angle can go to smaller values which are not responsible themselves for the rupture of the bonds. In fact, the smaller angles have to be accompanied by other factors such as the weakening and breaking of the O(1)-O(2) bond and the strengthening of the Au(2)-O(1) bond [see the inset of graph (a)]. The behavior of the β -angle is depicted in Fig. 5(b), where one can see the opening of this angle toward the value of 180° , which is the angle of the CO₂ molecule in the gas phase when the O(1)-O(2) bond breaks around frame C. Figure 5(c) shows the behavior of O(1), the oxygen attached to the Au atoms. As the O(2) breaks its bond with O(1), the Au(2)-O(1) bond distance shortens and becomes equal to the Au(3)-O(1) bond. The average Au(2)-O(1) bond distance depends on the stress of the NW. If this bond is larger due to stress, it hinders the occurrence of the reaction. Figure 5(d) shows the behavior of the O(1)-O(2) distance, which starts to increase in frame B, just before the increase of the Au(2)-C bond at frame C resulting in its breaking and the formation of a CO₂ molecule. Therefore, the CO₂ molecule leaves an atomic O impurity in the LAC NW.

IV. CONCLUSIONS

In conclusion, we used state-of-the-art computer simulations to perform DFT calculations (CG and finite-temperature AIMD) to study the reactivity of thin Au NWs. We presented a possible route for the formation of such atomic impurities

through a catalytic oxidation process involving O₂ and CO molecules resulting in a harmless CO₂ molecule and one atomic O impurity inserted into the LAC NW. We show that O₂ can be adsorbed on the LAC in different forms, depending on the degree of tension experienced by the NW. One of these situations (discussed in detail in Sec. III) describes a reaction where an O₂ molecule attaches only one of its O atoms to two Au LAC atoms. After this event, a CO molecule, that is nearby, can also attach to one Au LAC atom forming an O₂CO complex. Then a concerted evolution motion of this complex produces a CO₂ molecule that detaches from the LAC leaving a single atomic impurity in the Au LAC. This process might unveil the mystery of the origin of O atomic impurities in Au NWs. We hope that this study will prompt interesting experiments and also the search for other routes of chemical reactions that can be catalyzed by Au NWs.

ACKNOWLEDGMENTS

M.A.S. would like to thank CAPES for providing a grant to support a stay at the Institute of Physics “Gleb Wataghin” in UNICAMP. A.P.F.N. would like to thank CAPES for a Ph.D grant. This research had financial support from FAPESP (Project: 2010/16970-0), CNPq (Grant No. 304068/2011-0), CAPES (REDE NANOBIOTEC-BRASIL/ 04/2008), and FAPEX-UNICAMP. The calculations were performed at the National Center for High Performance Computing in Sao Paulo (CENAPAD-SP).

-
- [1] H. Ohnishi, Y. Kondo, and K. Takayanagi, *Nature (London)* **395**, 780 (1998).
 - [2] V. Rodrigues and D. Ugarte, *Phys. Rev. B* **63**, 073405 (2001).
 - [3] W. H. A. Thijssen, D. Marjenburgh, R. H. Bremmer, and J. M. van Ruitenbeek, *Phys. Rev. Lett.* **96**, 026806 (2006).
 - [4] T. Kizuka, *Phys. Rev. B* **77**, 155401 (2008).
 - [5] E. Z. da Silva, A. J. R. da Silva, and A. Fazzio, *Phys. Rev. Lett.* **87**, 256102 (2001).
 - [6] E. Z. da Silva, F. D. Novaes, A. J. R. da Silva, and A. Fazzio, *Phys. Rev. B* **69**, 115411 (2004).
 - [7] E. P. M. Amorim and E. Z. da Silva, *Phys. Rev. Lett.* **101**, 125502 (2008).
 - [8] E. Anglada, J. A. Torres, F. Yndurain, and J. M. Soler, *Phys. Rev. Lett.* **98**, 096102 (2007).
 - [9] F. D. Novaes, A. J. R. da Silva, E. Z. da Silva, and A. Fazzio, *Phys. Rev. Lett.* **90**, 036101 (2003).
 - [10] N. V. Skorodumova and S. I. Simak, *Phys. Rev. B* **67**, 121404(R) (2003).
 - [11] R. N. Barnett, H. Hakkinen, A. G. Scherbakov, and U. Landman, *Nanolett.* **4**, 1845 (2004).
 - [12] F. D. Novaes, E. Z. da Silva, A. J. R. da Silva, and A. Fazzio, *Appl. Phys. A* **81**, 1551 (2005).
 - [13] F. D. Novaes, A. J. R. da Silva, E. Z. da Silva, and A. Fazzio, *Phys. Rev. Lett.* **96**, 016104 (2006).
 - [14] M. Haruta, T. Kobayashi, H. Sano, and N. Yamada, *Chem. Lett.* **2**, 405 (1987).
 - [15] R. Coquet, K. L. Howard, and D. J. Willock, *Chem. Soc. Rev.* **37**, 2046 (2008).
 - [16] G. Huchings and M. Haruta, *Appl. Catal. A* **291**, 2 (2005).
 - [17] M. Valden, X. Lai, and D. W. Goodman, *Science* **281**, 1647 (1998).
 - [18] M. M. Schubert, S. Hackenberg, A. C. van Veen, M. Muhler, V. Plzak, and R. J. Behm, *J. Catal.* **197**, 113 (2001).
 - [19] A. Wolf and F. Schuth, *Appl. Catal. A* **226**, 1 (2002).
 - [20] M. Mavrikakis, P. Stoltze, and J. K. Norskov, *Catal. Lett.* **64**, 101 (2000).
 - [21] Z.-P. Liu, P. Hu, and A. Alavi, *J. Am. Chem. Soc.* **124**, 14770 (2002).
 - [22] Z.-P. Liu, X.-Q. Gong, J. Kohanoff, C. Sanchez, and P. Hu, *Phys. Rev. Lett.* **91**, 266102 (2003).
 - [23] L. M. Molina and B. Hammer, *Phys. Rev. Lett.* **90**, 206102 (2003).
 - [24] Y. Xu and M. Mavrikakis, *J. Phys. Chem. B* **107**, 9298 (2003).
 - [25] P. Frondelius, H. Hakkinen, and K. Honkala, *Angew. Chem. Int. Ed.* **49**, 7913 (2010).
 - [26] R. H. M. Smit, Y. Noat, C. Untiedt, N. D. Lang, M. C. van Hemert, and J. M. van Ruitenbeek, *Nature (London)* **419**, 906 (2002).
 - [27] P. Hohenberg and W. Kohn, *Phys. Rev.* **136**, B864 (1964).
 - [28] W. Kohn and L. J. Sham, *Phys. Rev.* **140**, A1133 (1965).
 - [29] J. P. Perdew, K. Burke, and M. Ernzerhof, *Phys. Rev. Lett.* **77**, 3865 (1996).
 - [30] N. Troullier and J. L. Martins, *Phys. Rev. B* **43**, 1993 (1991).
 - [31] P. Ordejón, E. Artacho, and J. M. Soler, *Phys. Rev. B* **53**, R10441 (1996).

- [32] D. Sánchez-Portal, P. Ordejón, E. Artacho, and J. M. Soler, *Int. J. Quantum Chem.* **65**, 453 (1997).
- [33] E. Artacho, D. Sanchez-Portal, P. Ordejon, A. Garcia, and J. M. Soler, *Phys. Status Solidi* **125**, 809 (1999).
- [34] H. J. Monkhorst and J. D. Pack, *Phys. Rev. B* **13**, 5188 (1976).
- [35] E. Hobi Jr., A. J. R. da Silva, F. D. Novaes, E. Z. da Silva, and A. Fazzio, *Phys. Rev. Lett.* **95**, 169601 (2005).
- [36] E. Hobi Jr., A. Fazzio, and A. J. R. da Silva, *Phys. Rev. Lett.* **100**, 056104 (2008).
- [37] Jmol: an open-source Java viewer for chemical structures in 3D. <http://www.jmol.org/>
- [38] See Supplemental Material at <http://link.aps.org/supplemental/10.1103/PhysRevB.89.085417> to view the videos that illustrate the AIMD simulations.
- [39] B. Yoon, H. Hakkinan, and U. Landman, *J. Phys. Chem. A* **107**, 4066 (2003).
- [40] G. A. Somorjai, *Introduction to Surface Chemistry and Catalysis* (Wiley, New York, 1994).